Yu et al. *NPG Asia Materials* (2018) 10: 882–887
DOI 10.1038/s41427-018-0081-y

NPG Asia Materials

ARTICLE Open Access

Unraveling a novel ferroelectric GeSe phase and its transformation into a topological crystalline insulator under high pressure

Hulei Yu[1,2], Dexiang Gao[3], Xiancheng Wang[4], Xueyan Du[3], Xiaohuan Lin[3], Wenhan Guo[5], Ruqiang Zou[5], Changqing Jin[4], Kuo Li[3] and Yue Chen[1,2]

Abstract

Germanium selenide is a promising material for electronic, photovoltaic, and thermoelectric applications; however, structural phase transitions of GeSe under pressure are controversial. Combining evolutionary algorithms, density functional theory, tight-binding method, and laser-heated diamond anvil cell experiments, pressure-induced phase transitions of GeSe are thoroughly investigated. Two novel intermediate phases are predicted to exist in between the well-known α-GeSe and the recently discovered β-GeSe under high pressure. α-GeSe is found to transform into a rhombohedral crystal structure with a space group of *R*3*m* at a low hydrostatic pressure. The *R*3*m* phase of GeSe exhibits robust ferroelectricity analogous to GeTe. By further increasing the pressure to approximately 6 GPa, the *R*3*m* phase is predicted to transform into a rock-salt structure, becoming a 3D topological crystalline insulator with an inverted band structure. The newly discovered GeSe high-pressure phases greatly enrich our knowledge of IV–VI compounds.

Introduction

The IV–VI binary compounds have attracted much research interest due to their promising photovoltaic and thermoelectric applications. For example, a SnSe single crystal was recently found to exhibit a record high thermoelectric figure of merit[1–3]. PbTe is an important material for photodetectors[4,5] and solar cells[6] that is also a well-known high-performance thermoelectric material because of its low thermal conductivity[7]. GeTe has a ferroelectric phase transition at approximately 670 K and is important for electronic memory applications[8]. Moreover, rock-salt SnTe[9] and SnSe[10,11] were found to be topological crystalline insulators (TCIs), in which the topological states are protected by crystal symmetry[12,13].

As a promising IV–VI compound, GeSe is a narrow band gap semiconductor and possesses an orthorhombic *Pnma* crystal structure (GeS-type) at ambient conditions[14]. Most existing studies focus on this laminar *Pnma* structure, whereas the properties and structural phase transitions of GeSe under pressure are largely unexplored. Until recently, it was unknown that a new β-GeSe phase exists under a hydrostatic pressure as low as 6 GPa[15]. The β phase still exists after recovering to ambient conditions and its electrical conductivity was found to be essentially temperature independent. Bhatia et al.[16] performed high-pressure experiments on single crystal GeSe, in which an abrupt drop in the electrical resistance at 6 GPa was observed because of the transformation to a face-centered-cubic phase. Nonetheless, Hsueh et al.[17] attributed the reduction of electrical resistance to the

Correspondence: Kuo Li (likuo@hpstar.ac.cn) or Yue Chen (yuechen@hku.hk)
[1]Department of Mechanical Engineering, The University of Hong Kong, Pokfulam Road, Hong Kong SAR, China
[2]HKU Zhejiang Institute of Research and Innovation, 1623 Dayuan Road, Lin An 311305, China
Full list of author information is available at the end of the article.

© The Author(s) 2018
Open Access This article is licensed under a Creative Commons Attribution 4.0 International License, which permits use, sharing, adaptation, distribution and reproduction in any medium or format, as long as you give appropriate credit to the original author(s) and the source, provide a link to the Creative Commons license, and indicate if changes were made. The images or other third party material in this article are included in the article's Creative Commons license, unless indicated otherwise in a credit line to the material. If material is not included in the article's Creative Commons license and your intended use is not permitted by statutory regulation or exceeds the permitted use, you will need to obtain permission directly from the copyright holder. To view a copy of this license, visit http://creativecommons.org/licenses/by/4.0/.

metallization of the α phase. It is obvious that a systematic study is imperative for a more complete understanding of the high-pressure behavior of GeSe.

New phases with interesting properties may exist under high pressures[18]; e.g., a novel intermediate phase of SnTe with the *Pnma* space group was recently discovered using angle-dispersive synchrotron X-ray diffraction[19]. Because high-pressure experimental characterizations are expensive and time-consuming, a theory-assisted ground state structural search is ideal for exploring potential new high-pressure phases[20,21]. Ab initio evolutionary algorithms were recently shown to be extremely powerful in new crystal structure predictions. This algorithm has been proven to be effective in finding the global minimum of the potential energy by mimicking Darwin's theory of evolution. Employing the natural selection of the fittest (e.g., the phases with the lowest potential energies in this work), a new generation can be generated using operators, such as heredity, soft mutation, and transmutation. The ground-state phases may be identified after a sufficient amount of generations. Details of the operators for generating new generations can be found in ref. [20]. By using this method, a transparent sodium high-pressure phase was predicted and later confirmed in experiments[22]; a metallic two-dimensional boron sheet was predicted and synthesized in the experiments[21]. In this work, we systematically investigate the GeSe compound under pressure from extensive evolutionary algorithm searches and laser-heated diamond anvil cell (DAC) experiments. Two new phases were found to exist in between the α and the β phases with intriguing properties.

Materials and methods

Computational details

Structure searches were performed by combining the evolutionary algorithms and density functional theory (DFT) as implemented in USPEX[23] and Vienna ab initio simulation package (VASP)[24]. The maximum number of atoms allowed in a unit cell was 18. All existing crystal structures of GeSe were taken into account in the evolutionary searches[25]. New generations were obtained using the following schemes: heredity (40%), random (20%), softmutation/coormutation (20%), and transmutation (20%). The projector augmented wave (PAW) method[26] combined with the generalized gradient approximation (GGA) of Perdew–Burke–Ernzerhof (PBE) functional[27] was applied. Forces and full stress tensors were calculated and used to relax crystal structures into their ground states. The Brillouin zones were meshed using the gamma-centered Monkhorst–Pack method[28] with a density of approximately $0.03 \times 2\pi$ Å^{-1}. A plane-wave energy cut-off of 350 eV was used and the convergence criterion of electronic self-consistent calculations was set to 10^{-6} eV. A large $4 \times 4 \times 4$ supercell of 128 atoms was adopted to study the phonon dispersions using the small displacement method[29]. The effect of longitudinal optical-transverse optical (LO-TO) splitting was considered in the phonon calculations. To ensure accurate phonon calculations, we applied a higher total energy convergence criterion of 10^{-8} eV.

Experimental details

A piece of α-GeSe sample, sandwiched between MgO for thermal insulation, was loaded in a DAC (diamond culet size $d = 400$ μm). The sample was compressed to ~2 GPa as calibrated by Ruby fluorescence under room temperature, and then double-sided heated to 1600 K for approximately 45 min using an ytterbium fiber laser with a wavelength of 1070 nm. The cell was then cooled down and the pressure was released. The sample was picked up from the gasket, and the X-ray powder diffraction (XRD) was measured using the powder mode of Rigaku XtaLab Pro X-ray single crystal diffractometer, under the voltage of 50 kV and the current of 24 mA, with Mo Kα as the X-ray source. Rietveld refinement was conducted using the Topas 3 program with the simulated annealing method.

Results

Two energetically preferable new phases were found in our ab initio evolutionary searches under pressure. As shown in Fig. 1a, GeSe has a sophisticated phase

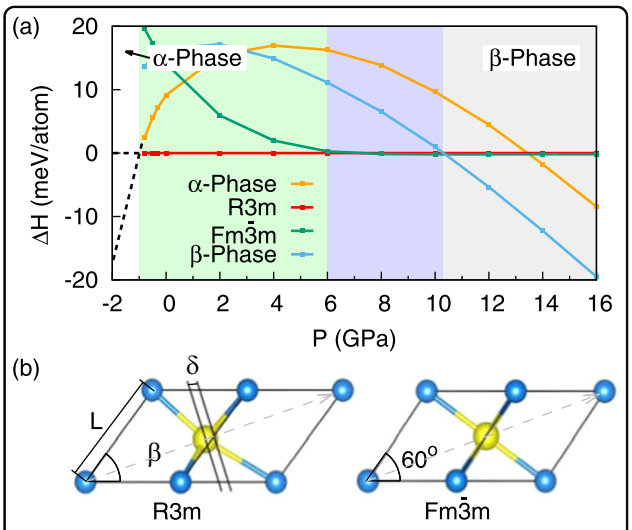

Fig. 1 Enthalpies of competing GeSe high-pressure phases and the crystal structures. a Enthalpy differences of the competing crystal structures of GeSe as functions of hydrostatic pressures. The dashed line represents an extrapolation of the enthalpy difference. **b** Primitive cells of the two intermediate phases that exist in between α- and β-GeSe. The blue and yellow spheres represent the Ge and Se atoms, respectively. The lattice constant, the angle between two lattice vectors, and the relative atomic displacement from the cell center are labeled with *L*, *β*, and *δ*, respectively. The dashed gray arrows indicate the [1 1 1] direction

transition path. With increasing pressure, GeSe transforms from the α phase through two intermediate phases of *R*3*m* and *Fm*$\bar{3}$*m* into the recently discovered β phase. Although the experimental phase transition pressures were not precisely reproduced (e.g., the ambient α phase is predicted to exist under a small negative pressure of approximately −1 GPa and the β phase is predicted to exist above 10 GPa, in contrast to the experimental 6 GPa[15]), the correct transition order from the α to the β phase is predicted. The differences between the exact values of theoretical and experimental phase transition pressures may be related to the complex high-pressure experimental conditions and the exclusion of vibrational entropy in DFT calculations. The newly predicted *R*3*m* phase has a trigonal layered crystal structure of the GeTe prototype and transforms into the *Fm*$\bar{3}$*m* phase with a rock-salt crystal structure at approximately 6 GPa. A similar pressure-induced displacive phase transition between *R*3*m* and *Fm*$\bar{3}$*m* was also observed in another IV–VI compound, GeTe[30], suggesting the robustness of our theoretical study.

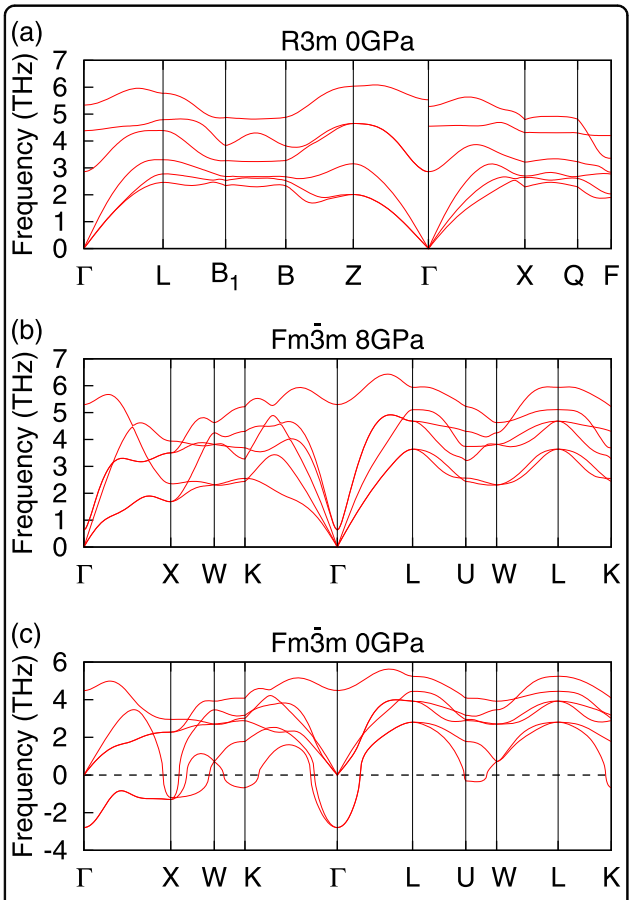

Fig. 2 Phonon dispersions of the different phases of GeSe at selected pressures. The negative values represent imaginary phonon frequencies

In addition to the energetics, the lattice dynamics of the *R*3*m* and *Fm*$\bar{3}$*m* phases are also investigated to examine the possibility of experimental synthesis. As shown in Fig. 2a, all phonon modes of the *R*3*m* phase have positive frequencies, indicating that this phase is dynamically stable. However, the *Fm*$\bar{3}$*m* phase only becomes dynamically stable under a suitable hydrostatic pressure (see Fig. 2b). At 0 GPa, a large number of phonon modes of the *Fm*$\bar{3}$*m* phase exhibit imaginary frequencies (see Fig. 2c), suggesting that this phase is dynamically unstable. These soft modes induce a phase transformation from the *Fm*$\bar{3}$*m* phase to the *R*3*m* phase at low pressures. As the external pressure is increased, the soft phonon modes are gradually hardened, consistent with previous DFT calculations[31]. Therefore, the *Fm*$\bar{3}$*m* phase only exists under suitable hydrostatic pressures.

To obtain more evidence for our newly predicted GeSe high-pressure phases, we have performed laser-heated DAC experiments. From the XRD pattern shown in Fig. 3, α-GeSe and MgO were unambiguously identified. Additionally, several extra diffraction peaks were observed, such as the two peaks indicated by arrows near 21°. By testing all of the competing crystal structures, we found that the *R*3*m* phase reasonably fits these peaks in the Rietveld refinement, suggesting that our theoretical prediction is robust. The refined lattice parameters and the molar fractions of the different phases are summarized in Table 1. It is seen that the experimental lattice parameters are in reasonable agreement with the DFT results. It is also noted that laser heating is critical for synthesizing the *R*3*m* phase of GeSe; the phase transition only occurs through melting and crystallization under pressure. Furthermore, a rhombohedral phase similar to our *R*3*m*

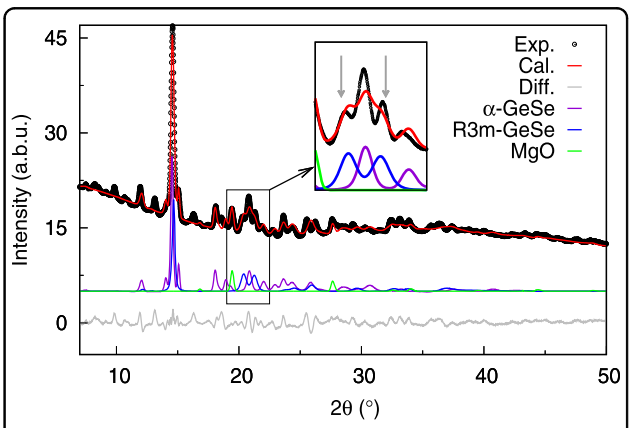

Fig. 3 Rietveld refinement of the GeSe sample recovered from 2 GPa and 1600 K. The black circles and red solid curves represent the experimental data and the simulated results, respectively. The purple, blue, green, and gray curves denote the contributions from α-GeSe, *R*3*m*-GeSe, MgO, and the differences between the experimental and the simulated results, respectively

Table 1 Refined crystal structure data from high-pressure DAC experiments and the lattice parameters calculated from DFT at 0 GPa

Phases	Molar ratio	Space group	Lattice parameters	DFT lattice parameters
R3m-GeSe	39%	*R3m*	$a = 3.87$ Å	$a = 3.95$ Å
			$c = 10.01$ Å	$c = 9.98$ Å
α-GeSe	37%	*Pnma*	$a = 4.30$ Å	$a = 4.49$ Å
			$b = 3.92$ Å	$b = 3.90$ Å
			$c = 10.81$ Å	$c = 11.20$ Å
MgO	24%	$Fm\bar{3}m$	$a = 4.20$ Å	–

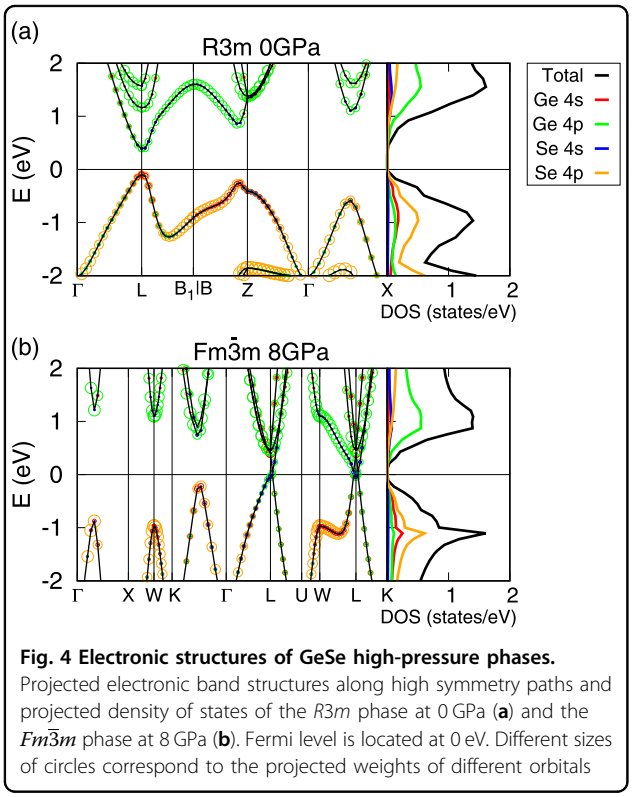

Fig. 4 Electronic structures of GeSe high-pressure phases. Projected electronic band structures along high symmetry paths and projected density of states of the *R3m* phase at 0 GPa (**a**) and the $Fm\bar{3}m$ phase at 8 GPa (**b**). Fermi level is located at 0 eV. Different sizes of circles correspond to the projected weights of different orbitals

phase was recently observed in GeSe–$AgSbSe_2$ alloys[32]. As alloying GeSe with $AgSbSe_2$ may be regarded as an internal chemical pre-compression, the observation of this rhombohedral phase represents additional indirect evidence for our work.

To better understand the newly discovered high-pressure phases of GeSe, their electronic band structures and density of states (DOS) were further studied. As shown in Fig. 4a, the *R3m* phase was found to be a semiconductor at 0 GPa with a direct band gap of approximately 0.49 eV near the high symmetry point, *L*. From the projected band structure and DOS, it was observed that the bottom of the conduction bands

Table 2 Lattice parameters (*L* and *β*), relative atomic displacements (*δ*), unit cell volumes (*V*), and the polarization densities (*P*) of *R3m*-GeSe and α-GeTe at 0 GPa

	L (Å)	*β* (°)	*δ* (Å)	*V* (Å^3)	*P* (μC/cm^2)
R3m-GeSe	4.14	57.41	0.35	47.33	65.73
α-GeTe	4.38	57.83	0.34	56.26	64.48
α-GeTe[43]	4.37	57.76	0.33	56.08	64.56

Polarization was calculated using Berry phase method

mainly consists of Ge 4*p* states, whereas the top of the valence bands is largely the Se 4*p* states. Most interestingly, the $Fm\bar{3}m$ phase has a gapless band structure at 8 GPa (see Fig. 4b). The gap is closed in the vicinity of the high symmetry point, *L*. Similar to the *R3m* phase, the electronic states of the $Fm\bar{3}m$ phase below the Fermi level are mostly attributed to the Se 4*p* states, with the main contribution to the electronic states above the Fermi level coming from the Ge 4*p* orbitals.

The *R3m* phase of GeSe has a similar crystal structure as α-GeTe and exhibits robust ferroelectricity[33–35]. The existence of the *R3m* phase makes GeSe distinctly different from most other IV–VI compounds. In contrast to the rock-salt crystal structure, the relative atomic displacement (RAD) of the Ge or Se atom along the [1 1 1] direction (see Fig. 1b) in the *R3m* phase results in a spontaneous polarization[36]. As a rule of thumb, the larger the RAD, the stronger the spontaneous polarization and the higher the ferroelectric transition temperature[37]. From DFT calculations (see Table 2), the RAD of *R3m*-GeSe is similar to that of α-GeTe implying a comparable ferroelectric transition temperature. Moreover, the ferroelectricity of *R3m*-GeSe is as robust as that of α-GeTe as demonstrated by their similar polarization densities. The ferroelectric nature of the newly discovered *R3m*-GeSe indicates potential applications in information storage and real-time optical processing[33,38]; however, a more efficient synthesis technique still needs to be developed.

The electronic band structure of the newly discovered $Fm\bar{3}m$ phase of GeSe was further studied. As shown in Fig. 5a, where the band structure was calculated without considering spin–orbit coupling (SOC), $Fm\bar{3}m$-GeSe has a gapless Dirac cone along the *L*–*W* path. After taking into account the SOC effects in our DFT calculations, we found that a band gap is opened, and the Dirac cone is broken consequently (see Fig. 5b). The $Fm\bar{3}m$ phase has an inverted band order around the *L* point, which cannot be broken by SOC, indicating that the $Fm\bar{3}m$ phase is different from that of the time-reversal Z_2 topological insulator. Furthermore, the band gap (E_L) at the high symmetry point, *L*, can be closed and reopened as the hydrostatic pressure increases from −8 to

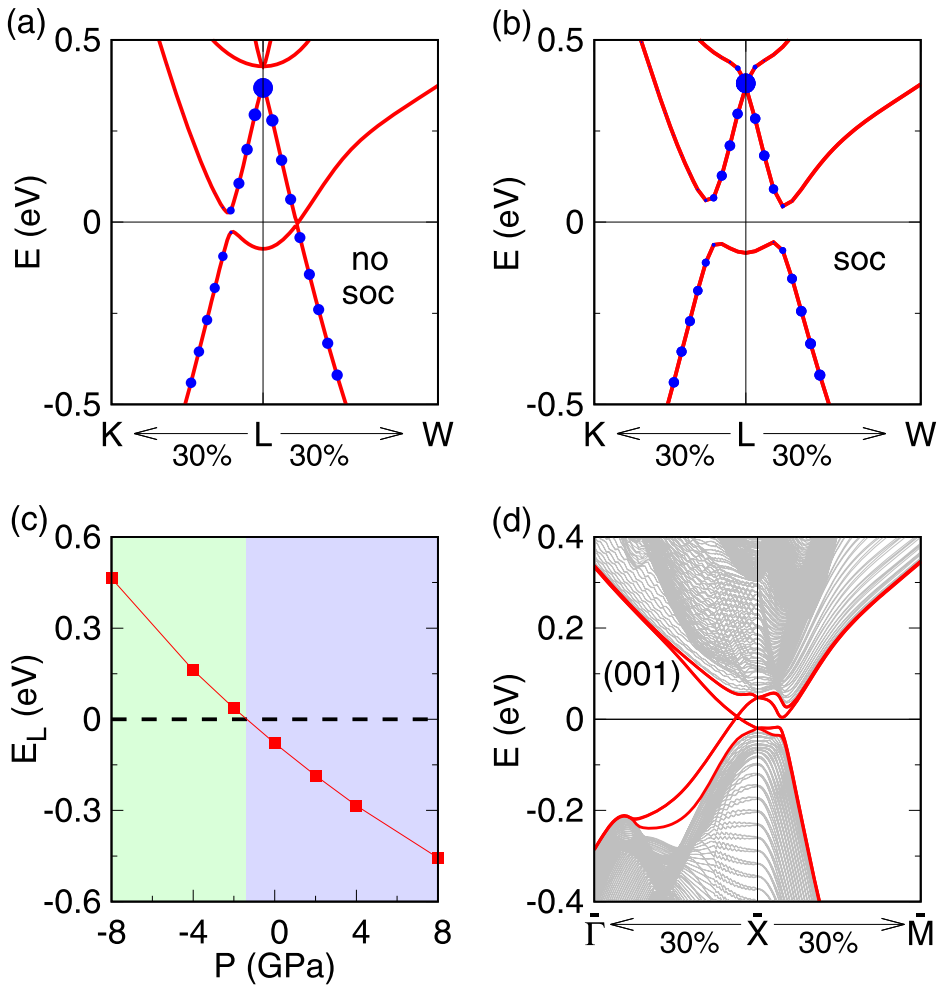

Fig. 5 Band inversion of the rock-salt GeSe phase. Electronic band structures of the $Fm\bar{3}m$ phase at 8 GPa calculated without SOC (**a**) and with SOC (**b**). The evolution of band gap at the high symmetry point, *L*, from DFT calculations with SOC (**c**). A negative gap represents that the bands are in an inverse order. The (001) surface band structure around $\bar{X}$ was calculated using the tight-binding method (**d**). The Fermi level is located at 0 eV. The size of the blue dots in panels (**a**) and (**b**) is proportional to the weight of the Ge 4*s* orbitals. The red curves in panel (**d**) represent the surface bands

8 GPa (see Fig. 5c). All these calculations imply a crystal-symmetry-driven nontrivial topological state. To explicitly define $Fm\bar{3}m$-GeSe as a TCI, the mirror Chern number n_M needs to be evaluated[12]. According to the k•p theory of band structure[39], the n_M of the mirror symmetry plane $(\bar{1}10)$ of the $Fm\bar{3}m$ phase changes its value by two when the pressure is increased from −8 to 8 GPa. Because $Fm\bar{3}m$-GeSe has no band inversion and is topologically trivial ($n_M = 0$) when the external pressure is equal to −8 GPa, the n_M is equal to −2 when a hydrostatic pressure of 8 GPa is applied. (The sign of n_M has been discussed in detail in ref. [40].) In addition, the (001) surface band structure is also calculated from a tight binding model, which is obtained utilizing the maximally localized Wannier functions[41,42]. A slab of 83 atomic layers was constructed to study the surface band structure. Figure 5d shows that a massless Dirac cone exists in the surface band structure along the $\bar{\Gamma} - \bar{X}$ path, demonstrating that $Fm\bar{3}m$-GeSe is a TCI under a hydrostatic pressure of 8 GPa.

Conclusions

The structural phase transitions of GeSe under hydrostatic pressures up to 16 GPa have been systematically studied from ab initio evolutionary structure searches. Two new phases with space groups of *R*3*m* and $Fm\bar{3}m$ are predicted to be stable in the pressure range between the α and the β phases. Laser-heated DAC experiments have been performed to provide evidence for the existence of the newly predicted *R*3*m* phase. It is found that *R*3*m*-GeSe has a layered crystal structure and exhibits robust ferroelectricity with a large spontaneous polarization. Under further compression, the *R*3*m* phase continuously transforms into the $Fm\bar{3}m$ phase. Phonon dispersion calculations show that this phase is dynamically stable at pressures above 8 GPa. Detailed electronic band structure studies reveal that the

$Fm\bar{3}m$ phase is a TCI. The intriguing properties of the newly discovered GeSe phases further enrich our knowledge on the high-pressure behaviors of IV–VI compounds.

Acknowledgements
This work is supported by the Research Grants Council of Hong Kong under project numbers 27202516 and 17200017, and the National Natural Science Foundation of China under project number 51706192. We are grateful for the research computing facilities offered by ITS, HKU. The authors thank Peijie Zhang for sample loading.

Author details
[1]Department of Mechanical Engineering, The University of Hong Kong, Pokfulam Road, Hong Kong SAR, China. [2]HKU Zhejiang Institute of Research and Innovation, 1623 Dayuan Road, Lin An 311305, China. [3]Center for High Pressure Science and Technology Advanced Research, 10 Dongbeiwang West Road, Beijing 100094, China. [4]Institute of Physics, Chinese Academy of Sciences, Beijing 100190, China. [5]Department of Materials Science and Engineering, Peking University, Beijing 100871, China

Author contributions
Y.C. proposed the investigation. H.L.Y. conducted the structural predictions and the calculations of the various properties of the GeSe phases. H.L.Y. and Y.C. analyzed the computational results. D.X.G., X.C.W., X.Y.D., X.H.L., W.H.G., R.Q.Z., C.Q.J. and K.L. performed the high pressure experiments and analyzed the XRD results. All authors reviewed the manuscript.

Conflict of interest
The authors declare that they have no conflict of interest.

Publisher's note
Springer Nature remains neutral with regard to jurisdictional claims in published maps and institutional affiliations.

Received: 18 March 2018 Revised: 3 July 2018 Accepted: 22 July 2018.
Published online: 7 September 2018

References

1. Zhao, L.-D. et al. Ultralow thermal conductivity and high thermoelectric figure of merit in SnSe crystals. *Nature* **508**, 373–377 (2014).
2. Zhao, L.-D. et al. Ultrahigh power factor and thermoelectric performance in hole-doped single-crystal SnSe. *Science* **351**, 141–144 (2016).
3. Yu, H., Dai, S. & Chen, Y. Enhanced power factor via the control of structural phase transition in SnSe. *Sci. Rep.* **6**, 26193 (2016).
4. Han, Z. et al. On-chip chalcogenide glass waveguide-integrated mid-infrared PbTe detectors. *Appl. Phys. Lett.* **109**, 071111 (2016).
5. Zhang, X., Yang, Z. & Chen, Y. Novel two-dimensional ferroelectric PbTe under tension: a first-principles prediction. *J. Appl. Phys.* **122**, 064101 (2017).
6. Böhm, M. L. et al. Lead telluride quantum dot solar cells displaying external quantum efficiencies exceeding 120%. *Nano Lett.* **15**, 7987–7993 (2015).
7. Shiga, T. et al. Microscopic mechanism of low thermal conductivity in lead telluride. *Phys. Rev. B* **85**, 155203 (2012).
8. Bruns, G. et al. Nanosecond switching in GeTe phase change memory cells. *Appl. Phys. Lett.* **95**, 043108 (2009).
9. Tanaka, Y. et al. Experimental realization of a topological crystalline insulator in SnTe. *Nat. Phys.* **8**, 800–803 (2012).
10. Sun, Y. et al. Rocksalt SnS and SnSe: native topological crystalline insulators. *Phys. Rev. B* **88**, 235122 (2013).
11. Wang, Z. et al. Molecular beam epitaxy-grown SnSe in the rock-salt structure: an artificial topological crystalline insulator material. *Adv. Mater.* **27**, 4150–4154 (2015).
12. Fu, L. Topological crystalline insulators. *Phys. Rev. Lett.* **106**, 106802 (2011).
13. Xu, S.-Y. et al. Observation of a topological crystalline insulator phase and topological phase transition in $Pb_{1-x}Sn_xTe$. *Nat. Commun.* **3**, 1192 (2012).
14. Wiedemeier, H. & von Schnering, H. G. Refinement of the structures of GeS, GeSe, SnS and SnSe. *Z. Kristallogr. Cryst. Mater.* **148**, 295–304 (1978).
15. von Rohr, F. O. et al. High-pressure synthesis and characterization of β-GeSe—a six-membered-ring semiconductor in an uncommon boat conformation. *J. Am. Chem. Soc.* **139**, 2771–2777 (2017).
16. Bhatia, K. L., Gosain, D. P., Parthasarathy, G. & Gopal, E. S. R. Pressure-induced first-order transition in layered crystalline semiconductor GeSe to a metallic phase. *Phys. Rev. B* **33**, 1492–1494 (1986).
17. Hsueh, H. C., Vass, H., Clark, S. J., Ackland, G. J. & Crain, J. High-pressure effects in the layered semiconductor germanium selenide. *Phys. Rev. B* **51**, 16750–16760 (1995).
18. Yu, H., Lao, W., Wang, L., Li, K. & Chen, Y. Pressure-stabilized tin selenide phase with an unexpected stoichiometry and a predicted superconducting state at low temperatures. *Phys. Rev. Lett.* **118**, 137002 (2017).
19. Zhou, D., Li, Q., Ma, Y., Cui, Q. & Chen, C. Unraveling convoluted structural transitions in SnTe at high pressure. *J. Phys. Chem. C* **117**, 5352–5357 (2013).
20. Oganov, A. R., Ma, Y., Lyakhov, A. O., Valle, M. & Gatti, C. Evolutionary crystal structure prediction as a method for the discovery of minerals and materials. *Rev. Mineral. Geochem.* **71**, 271–298 (2010).
21. Mannix, A. J. et al. Synthesis of borophenes: anisotropic, two-dimensional boron polymorphs. *Science* **350**, 1513–1516 (2015).
22. Ma, Y. et al. Transparent dense sodium. *Nature* **458**, 182–185 (2009).
23. Lyakhov, A. O., Oganov, A. R. & Valle, M. Crystal structure prediction using evolutionary approach. In: *Modern Methods of Crystal Structure Prediction* 147–180 Wiley-VCH, Weinheim (2010).
24. Kresse, G. & Furthmüller, J. Efficiency of ab-initio total energy calculations for metals and semiconductors using a plane-wave basis set. *Comput. Mater. Sci.* **6**, 15–50 (1996).
25. Oganov, A. R., Lyakhov, A. O. & Valle, M. How evolutionary crystal structure prediction works—and why. *Acc. Chem. Res.* **44**, 227–237 (2011).
26. Blöchl, P. E. Projector augmented-wave method. *Phys. Rev. B* **50**, 17953 (1994).
27. Perdew, J. P., Burke, K. & Ernzerhof, M. Generalized gradient approximation made simple. *Phys. Rev. Lett.* **77**, 3865 (1996).
28. Monkhorst, H. J. & Pack, J. D. Special points for brillouin-zone integrations. *Phys. Rev. B* **13**, 5188 (1976).
29. Togo, A., Oba, F. & Tanaka, I. First-principles calculations of the ferroelastic transition between rutile-type and $CaCl_2$-type SiO_2 at high pressures. *Phys. Rev. B* **78**, 134106 (2008).
30. Onodera, A., Sakamoto, I., Fujii, Y., Mori, N. & Sugai, S. Structural and electrical properties of GeSe and GeTe at high pressure. *Phys. Rev. B* **56**, 7935–7941 (1997).
31. Deringer, V. L., Stoffel, R. P. & Dronskowski, R. Vibrational and thermodynamic properties of GeSe in the quasiharmonic approximation. *Phys. Rev. B* **89**, 094303 (2014).
32. Huang, Z. et al. High thermoelectric performance of new rhombohedral phase of GeSe stabilized via alloying with $AgSbSe_2$. *Angew. Chem. Int. Ed.* **56**, 14113–14118 (2017).
33. Ciucivara, A., Sahu, B. R. & Kleinman, L. Density functional study of the effect of pressure on the ferroelectric GeTe. *Phys. Rev. B* **73**, 214105 (2006).
34. Boschker, J. E., Wang, R. & Calarco, R. GeTe: a simple compound blessed with a plethora of properties. *CrystEngComm* **19**, 5324–5335 (2017).
35. Kolobov, A. et al. Ferroelectric switching in epitaxial GeTe films. *APL Mater.* **2**, 066101 (2014).
36. Marcus, L. et al. Giant rashba-type spin splitting in ferroelectric GeTe(111). *Adv. Mater.* **28**, 560–565 (2016).
37. Fei, R., Kang, W. & Yang, L. Ferroelectricity and phase transitions in monolayer group-IV monochalcogenides. *Phys. Rev. Lett.* **117**, 097601 (2016).
38. Akola, J. & Jones, R. O. Structure of amorphous $Ge_8Sb_2Te_{11}$:GeTe–Sb_2Te_3 alloys and optical storage. *Phys. Rev. B* **79**, 134118 (2009).
39. Hsieh, T. H. et al. Topological crystalline insulators in the SnTe material class. *Nat. Commun.* **3**, 982 (2012).
40. Teo, J. C. Y., Fu, L. & Kane, C. L. Surface states and topological invariants in three-dimensional topological insulators: application to $Bi_{1-x}Sb_x$. *Phys. Rev. B* **78**, 045426 (2008).
41. Mostofi, A. A. et al. wannier90: A tool for obtaining maximally-localised wannier functions. *Comput. Phys. Commun.* **178**, 685–699 (2008).
42. Wu, Q., Zhang, S., Song, H.-F., Troyer, M. & Soluyanov, A. A. WannierTools: an open-source software package for novel topological materials. *Comput. Phys. Commun.* **224**, 405–416 (2018).
43. Di Sante, D., Barone, P., Bertacco, R. & Picozzi, S. Electric control of the giant rashba effect in bulk GeTe. *Adv. Mater.* **25**, 509–513 (2013).